

Bayesian Transfer Learning for Enhanced Estimation and Inference

Daoyuan Lai¹, Oscar Hernan Madrid Padilla², and Tian Gu^{3,*}

¹*Department of Statistics and Actuarial Science, University of Hong Kong*

²*Department of Statistics, University of California, Los Angeles*

³*Department of Biostatistics, Columbia University Mailman School of Public Health*

**Corresponding author: tg2880@cumc.columbia.edu*

Abstract

Transfer learning enhances model performance in a target population with limited samples by leveraging knowledge from related studies. While many works focus on improving predictive performance, challenges of statistical inference persist. Bayesian approaches naturally offer uncertainty quantification for parameter estimates, yet existing Bayesian transfer learning methods are typically limited to single-source scenarios or require individual-level data. We introduce TRansfer leArning via guided horseshoE prioR (TRADER), a novel approach enabling multi-source transfer through pre-trained models in high-dimensional linear regression. TRADER shrinks target parameters towards a weighted average of source estimates, accommodating sources with different scales. Theoretical investigation shows that TRADER achieves faster posterior contraction rates than standard continuous shrinkage priors when sources align well with the target while preventing negative transfer from heterogeneous sources. The analysis of finite-sample marginal posterior behavior reveals that TRADER achieves desired frequentist coverage probabilities, even for coefficients with moderate signal strength—a scenario where standard continuous shrinkage priors struggle. Extensive numerical studies and a real-data application estimating the association between blood glucose and insulin use in the Hispanic diabetic population demonstrate that TRADER improves estimation and inference accuracy over continuous shrinkage priors using target data alone, while outperforming a state-of-the-art transfer learning method that requires individual-level data.

Keywords: Data heterogeneity, global-local shrinkage prior, high-dimensional inference, transfer learning, sparsity

1 Introduction

In the era of big data, many advanced statistical methods rely on large, diverse datasets to achieve optimal performance. However, in high-dimensional settings, particularly when working with underrepresented populations, obtaining sufficient data can be challenging. For example, fine-mapping is a technique in statistical genetics that seeks to identify causal variants linked to diseases. It often struggles with small sample sizes, weak variant signals, or low allele frequencies in underrepresented populations (Schaid et al., 2018; Li et al., 2024). These challenges are further exacerbated in populations with complex genetic structures, where fine-mapping suffers from inadequate linkage disequilibrium information. To overcome these limitations, researchers have explored integrating data with larger sample sizes and more comprehensive genomic data to improve statistical power (Gao and Zhou, 2024). This approach highlights the potential of transfer learning, which extends this idea by enabling models to leverage information from related but distinct datasets to address data scarcity and enhance statistical performance, particularly for underrepresented groups. As one of the data integration techniques (Chatterjee et al., 2016; Han and Lawless, 2019), transfer learning has proven effective in enhancing model performance for underrepresented populations. Its applications extend beyond fine-mapping to various domains, including risk prediction (Cheng et al., 2019; Gu et al., 2022b; Li et al., 2023a; Gu et al., 2023a; Lu et al., 2024; Cai et al., 2024), classification (Al-Stouhi and Reddy, 2016), and others (Gu et al., 2019; Jin and Yin, 2021; Zhang and Yin, 2023; Gu et al., 2023b,c). By transferring knowledge from larger or more comprehensive datasets (*sources*), transfer learning improves model

performance in a target population (*target*) where data is limited.

Recently, transfer learning has attracted considerable attention in the context of high-dimensional linear regression. [Bastani \(2021\)](#) explored estimation and prediction using a single source dataset, while [Li et al. \(2022\)](#) extended this to handle multiple sources with varying similarities. [Tian and Feng \(2023\)](#) and [Li et al. \(2023b\)](#) further refined transfer learning for generalized linear models with relaxed assumptions. These methods generally assume (i) the availability of individual-level data across studies and (ii) that the difference between source and target estimates can be measured using a distance-based metric, such as ℓ_1 or ℓ_2 -norm. To relax the former assumption and address data-sharing constraints in practice, federated algorithms have been developed ([Duan et al., 2018, 2020, 2022](#); [Cai et al., 2022](#); [Li et al., 2023a](#); [Chen et al., 2024](#); [Lu et al., 2024](#)), enabling collaborative learning without direct data sharing. These methods, however, rely on robust collaborative infrastructure, efficient computation, and timely information exchange. On the contrary, pre-trained models from source studies provide a more flexible and accessible alternative. Methods that leverage pre-trained models, such as estimated regression parameters ([Zhai and Han, 2022](#); [Taylor et al., 2023](#); [Gu et al., 2023a](#); [Han et al., 2023](#)), offer a practical and appealing solution. Moreover, recent studies have highlighted the limitations of the latter assumption in handling cases where the target and source data differ significantly in scale ([Gu et al., 2022a](#)), a challenge frequently encountered in mixed-type outcome integration ([Miglioretti, 2003](#)) and cross-population data integration ([Need and Goldstein, 2009](#)). These findings highlight the need for innovative approaches to address such heterogeneity effectively.

Despite recent advancements, a key challenge in high-dimensional transfer learning lies in reliable parameter estimation and inference. Frequentist methods often rely on debiased

estimates to construct asymptotic normalities (Zhang and Zhang, 2014; van de Geer et al., 2014; Javanmard and Montanari, 2014), while Bayesian approaches use shrinkage priors to adapt to sparsity and provide credible intervals that adjust to unknown levels of sparsity (Carvalho et al., 2009, 2010). Bhadra et al. (2019) claimed that frequentist methods tend to maintain “honesty,” ensuring credible intervals achieve nominal coverage across the entire parameter space. However, this often comes at the expense of wider intervals. In contrast, Bayesian methods focus on “adaptation,” yielding narrower credible intervals that adapt to the underlying sparsity but may struggle with valid coverage in certain scenarios. In particular, Li (1989) demonstrated the inherent trade-off, showing it is impossible to build credible sets that are both honest and adaptative, highlighting the complementary strengths of frequentist and Bayesian paradigms in uncertainty quantification.

The Bayesian paradigm is well-suited for transfer learning as it allows prior information from external sources to be integrated into current inferences (Suder et al., 2023). However, existing Bayesian transfer learning methods face many limitations. Hickey et al. (2024) introduced a random effect calibration method that focuses on calibrating the target posterior predictive credible sets using the source, but it is restricted to a setting with low-dimensional data and a single informative source with individual-level data. Abba et al. (2024) applied a horseshoe prior on the ℓ_2 distance between target and source estimates, focusing on prediction. However, their method is restricted to single-source settings and requires individual-level data, limiting its applicability to scenarios with multiple sources or summary-level data. Additionally, their method is constrained to the normal-means model and can not be directly applied to linear model (Song and Liang, 2023). Zhang et al. (2024) proposed a conditional spike-and-slab (SSL) prior (Ishwaran and Rao, 2005) to handle cases

of partial information sharing, where a subset of covariates is shared between source and target datasets. However, their method also depends on individual-level source data, and lacks statistical inference procedures. More importantly, SSL is known to be highly sensitive to the specification of the number of non-zero coefficients (Zhang et al., 2022; Li et al., 2024).

The limitation of SSL prior motivates the use of continuous (or global-local) shrinkage priors, such as horseshoe priors (Carvalho et al., 2009; Polson and Scott, 2011). It is often desired that the credible interval of continuous shrinkage prior can achieve nominal coverage probability in the frequentist sense. However, van der Pas et al. (2017) and Wu et al. (2023) showed that while horseshoe priors provide good frequentist coverage for coefficients near zero or beyond a certain threshold, they tend to overshrinkage coefficients of moderate signal strength, causing undercoverage of the corresponding credible interval. Addressing this limitation is critical for ensuring robust inference and reliable uncertainty quantification in high-dimensional settings.

To address these gaps, we propose a novel Bayesian transfer learning method, which builds on the continuous shrinkage priors and leverages multiple source estimates from pre-trained models to improve estimation and inference in a target population with limited samples. By incorporating robust priors, our approach accommodates differences in scale between source and target parameters and mitigates the risk of performance degradation when source information is less relevant. Our key contributions include:

- **Safe and communication-efficient multi-source data integration:** Our framework leverages multiple source datasets to improve estimation in a target population with limited samples. It ensures privacy by not requiring the patient-level data and

is communication-efficient, as it only requires parameter estimates from pre-trained models using source datasets.

- **Robust Bayesian transfer learning with theoretical guarantees:** Compared to using target data alone, the proposed method provides credible intervals with more accurate estimates, proper frequentist coverage probabilities, and improved inference efficiency. Finite-sample theoretical guarantees show that the framework achieves optimal posterior contraction rates when the sources are well-aligned with the target and it remains robust in the worst-case scenario where the sources are significantly heterogeneous (i.e., uninformative to the target).

The structure of the paper is as follows. After introducing the proposed method in Section 2 and discussing its theoretical properties in Section 3, we show the results of extensive simulation studies to validate its performance in Section 4. In Section 5, we apply the proposed method to estimate the association between blood glucose level and long-term insulin usage in individuals with diabetes, followed by discussions in Section 6.

2 The Proposed Bayesian Transfer Learning Method

Suppose we have a target dataset $\mathcal{D}^{(0)} = (\mathbf{X}^{(0)}, \mathbf{y}^{(0)})$, where $\mathbf{X}^{(0)} \in \mathbb{R}^{n_0 \times p}$ is the p -dimensional covariate of size n_0 and $\mathbf{y}^{(0)} \in \mathbb{R}^{n_0}$ is the outcome of interest. We model the relationship between $\mathbf{X}^{(0)}$ and $\mathbf{y}^{(0)}$ through a linear model

$$y_i^{(0)} = \mathbf{x}_i^{(0)\top} \boldsymbol{\beta} + \epsilon_i^{(0)}, \quad (1)$$

where $\mathbf{x}_i^{(0)}$ is the i -th row of $\mathbf{X}^{(0)}$ and $y_i^{(0)}$ is the i -th element of $\mathbf{y}^{(0)}$, for $i = 1, \dots, n_0$, and the error term $\epsilon_i^{(0)}$ are independently normal distributed with zero mean and σ_0^2 variance. We assume $\boldsymbol{\beta} = (\beta_1, \dots, \beta_p)^\top \in \mathbb{R}^p$ is sparse, meaning the number of nonzero elements, s , is much smaller than p . We use a superscript $*$ in the parameters to denote their true values in the frequentist sense, and $\|\cdot\|_1$ and $\|\cdot\|$ to represent the ℓ_1 and ℓ_2 norm, respectively. Note that the norm calculations exclude the intercept term.

In addition, there are K independent source datasets $\mathcal{D}^{(k)} = (\mathbf{X}^{(k)}, \mathbf{y}^{(k)})$, $k = 1, \dots, K$, which may provide useful information for the estimation of $\boldsymbol{\beta}$, where $\mathbf{X}^{(k)} \in \mathbb{R}^{n_k \times p}$ and $\mathbf{y}^{(k)} \in \mathbb{R}^{n_k}$ of size n_k . $\mathbf{X}^{(k)}$ represents the same covariates as $\mathbf{X}^{(0)}$, while $\mathbf{y}^{(k)}$ may represent the same outcome as $\mathbf{y}^{(0)}$ or a related one. The source model for the k -th source dataset satisfies

$$g^{(k)}[\mathbb{E}(y_i^{(k)})] = \mathbf{x}_i^{(k)\top} \boldsymbol{\omega}^{(k)},$$

where $\boldsymbol{\omega}^{(k)}$ are the source coefficients, $g^{(k)}$ is the link function corresponding to the type of $y_i^{(k)}$. To create a more practical and privacy-preserving framework and address real-world data-sharing restrictions, we assume access only to source estimates $\widehat{\boldsymbol{\omega}}^{(k)}$ rather than patient-level data. When $\boldsymbol{\beta}$ and $\boldsymbol{\omega}^{(k)}$'s share certain similarities, we want to transfer useful information from $\widehat{\boldsymbol{\omega}}^{(k)}$'s to guide the estimation of $\boldsymbol{\beta}$, with appropriate uncertainty quantification.

2.1 A Robust Two-Step Procedure to Leverage Multiple Unequal-Scaled Source Estimates

TRADER consists of a robust two-step procedure to handle cases where source and target estimates are concordant but differ in scale. As seen from Figure 1(A), the traditional distance-based transfer learning methods that use ℓ_2 norm to quantify β and $\omega^{(k)}$ essentially rely on $\omega^{(k)}$ to span a ball-shaped space, guiding the estimation of β , with h serving as the radius of the ball centered around $\omega^{(k)}$. We see that when the distance, h , between the two vectors becomes large, the ball-space may not provide sufficient guidance for learning the target β , which is common when $\omega^{(k)}$ is of unequal scale from β . We propose two steps to address this and illustrate them in Figure 1(B):

Step 1: Re-scaling each source estimate. We re-scale each source estimate $\hat{\omega}^{(k)}$ to a similar scale as β through the scaling factors $\|\hat{\beta}^{\text{val}}\|/\|\hat{\omega}^{(k)}\|$. The estimate $\hat{\beta}^{\text{val}}$ is calculated using an independent validation dataset, which can be a small subset split from the target data that will not be used in subsequent model training or evaluation. Throughout this paper, we randomly select 1/3 of the target data as an independent dataset to compute $\hat{\beta}^{\text{val}}$.

Step 2: Adaptive weighting to combine multiple sources. To leverage information from multiple source estimates, we compute a weighted average of all K source estimates, $\sum_{k=1}^K \eta_k \hat{\omega}^{(k)}$, by adaptively adjusting the weights, η_k . The weights are determined based on how similar the sources are to the target parameter. We use cosine similarity between the source and the target estimate to determine how informative each source is, giving higher weights to the more informative sources. The specific process will be discussed in the following section.

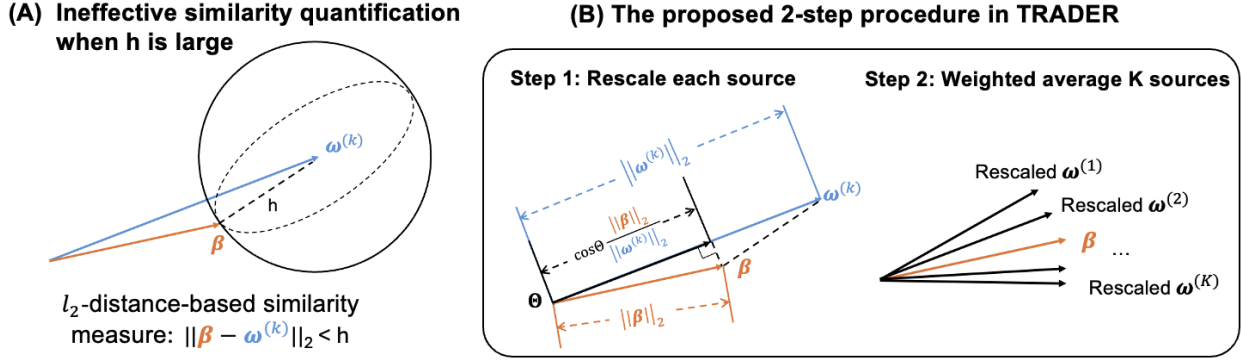


Figure 1: Schematic illustration of an existing challenge and the proposed two-step procedure. (A) When the scale of the target model parameter β and the k -th source parameter $\omega^{(k)}$ are different, the ℓ_2 -distance-based similarity measure spans a large ball space, which may be ineffective in leveraging the source information to estimate β ; and (B) the proposed 2-step procedure to combine multiple unequal-scaled source estimates in TRADER.

2.2 The Source-guided Horseshoe Prior

The steps 1-2 are implemented through the following prior on $\beta_j, j \in \{1, \dots, p\}$:

$$\beta_j \sim \mathcal{N} \left(\sum_{k=1}^K \eta_k \frac{\|\widehat{\beta}^{\text{val}}\|}{\|\widehat{\omega}^{(k)}\|} \widehat{\omega}_j^{(k)} + \eta_{K+1} \cdot 0, \quad \sigma^2 \lambda_j^2 \tau^2 \right),$$

$$(\eta_1, \dots, \eta_K, \eta_{K+1}) \sim \text{Dirichlet}(\theta_1, \dots, \theta_K, \zeta),$$

$$\lambda_j \sim \text{Cauchy}^+(0, 1),$$

$$\sigma^2 \sim \text{Inverse-Gamma}(\nu, \nu).$$
(2)

We refer to Equation (2) as a *source-guided horseshoe prior* because, unlike the standard horseshoe prior (with a prior mean of zero), the proposed prior has a mean adaptively informed by source datasets. The prior mean consists of two parts, a weighted average of the rescaled source estimates with $\|\widehat{\beta}^{\text{val}}\|/\|\widehat{\omega}^{(k)}\|$ as the scaling factor introduced in step 1, and a η_{K+1} -weighted zero mean. TRADER assigns greater weight to the more informative sources, leveraging their information to estimate β . To achieve this, we apply a Dirichlet

prior to the weights $(\eta_1, \dots, \eta_K, \eta_{K+1})$, where η_k 's are informed by the cosine similarity $\theta_k = \widehat{\boldsymbol{\omega}}^{(k)\top} \widehat{\boldsymbol{\beta}}^{\text{val}} / (\|\widehat{\boldsymbol{\omega}}^{(k)}\| \|\widehat{\boldsymbol{\beta}}^{\text{val}}\|)$ and $\zeta = 1$. Thus, sources with larger cosine similarity values receive greater weight, enabling TRADER to leverage informative sources effectively. In the extreme case where all sources are uninformative and heterogeneous from the target, it will yield relatively small θ_k values and the prior mass will concentrate on η_{K+1} , causing TRADER to revert to a standard horseshoe prior with zero prior mean, thus preventing negative transfer.

For other parameters, we set a standard half-Cauchy prior for the local shrinkage parameter λ_j , an inverse Gamma prior with $\nu = 0.01$ for the variance term σ^2 , and the choice of global shrinkage parameter τ is discussed in Section 2.4.

2.3 Posterior Distribution of TRADER

We show that the posterior mean of TRADER is a weighted average between the target and source estimates. To illustrate, we first consider the case of a single source estimator $\widehat{\boldsymbol{\omega}}^{(1)}$. Given the target data $\mathcal{D}^{(0)}$, $\widehat{\boldsymbol{\omega}}^{(1)}$, and hyperparameters, the posterior distribution of TRADER can be expressed as

$$\pi(\boldsymbol{\beta} \mid \tau, \boldsymbol{\Lambda}, \widehat{\boldsymbol{\omega}}, \mathcal{D}^{(0)}) \sim \mathcal{N}(\widehat{\boldsymbol{\beta}}, \widehat{\boldsymbol{\Sigma}}), \text{ where} \quad (3)$$

$$\begin{cases} \widehat{\boldsymbol{\beta}} = \tau^2 \boldsymbol{\Lambda} [\tau^2 \boldsymbol{\Lambda} + (\mathbf{X}^{(0)\top} \mathbf{X}^{(0)})^{-1}]^{-1} \widehat{\boldsymbol{\beta}}^{\text{OLS}} + (\tau^2 \boldsymbol{\Lambda} \mathbf{X}^{(0)\top} \mathbf{X}^{(0)} + \mathbf{I})^{-1} \widetilde{\boldsymbol{\omega}}^{(1)} \\ \widehat{\boldsymbol{\Sigma}} = \sigma_0^2 (\mathbf{X}^{(0)\top} \mathbf{X}^{(0)} + \tau^{-2} \boldsymbol{\Lambda}^{-1})^{-1} \end{cases}$$

with $\boldsymbol{\Lambda} = \text{diag}(\lambda_1^2, \dots, \lambda_p^2)$, $\widehat{\boldsymbol{\beta}}^{\text{OLS}} = (\mathbf{X}^{(0)\top} \mathbf{X}^{(0)})^{-1} \mathbf{X}^{(0)\top} \mathbf{y}^{(0)}$ as the ordinary least squared (OLS) estimate if $(\mathbf{X}^{(0)\top} \mathbf{X}^{(0)})^{-1}$ exists, and the scaled source parameter $\widetilde{\boldsymbol{\omega}}^{(1)} = (\|\widehat{\boldsymbol{\beta}}^{\text{val}}\| / \|\widehat{\boldsymbol{\omega}}^{(1)}\|) \widehat{\boldsymbol{\omega}}^{(1)}$.

When the columns of $\mathbf{X}^{(0)}$ are uncorrelated with zero mean and unit variance, we have $\mathbf{X}^{(0)\top}\mathbf{X}^{(0)} \approx n_0\mathbf{I}$, and we can approximate the j -th element of $\widehat{\boldsymbol{\beta}}$ as a weighted average of the j -th element of $\widehat{\boldsymbol{\beta}}^{\text{OLS}}$ and $\widetilde{\boldsymbol{\omega}}^{(1)}$

$$\widehat{\beta}_j = (1 - \kappa_j) \widehat{\beta}_j^{\text{OLS}} + \kappa_j \widetilde{\omega}_j^{(1)}, \quad (4)$$

where the weight of the source is $\kappa_j = 1/(1 + \tau^2 \lambda_j^2 n_0)$.

Equation (4) indicates that the posterior of TRADER estimator is a weighted average of $\widehat{\boldsymbol{\beta}}^{\text{OLS}}$ and $\widetilde{\boldsymbol{\omega}}^{(1)}$, where the degree of proximity towards source is determined by κ_j . For multiple source estimates, the results extend by replacing the single source estimate with a weighted average of multiple source estimates, $\sum_{k=1}^K \eta_k \widetilde{\boldsymbol{\omega}}^{(k)}$. The weighted average form of TRADER estimator is consistent with findings in other transfer learning methods, where the target-source similarity is measured by various distance-based similarity metrics, such as ℓ_2 norm (Gu et al., 2024) or Kullback-Leibler divergence (Hector and Martin, 2024).

2.4 Choice of the Global Parameter

Equation (4) indicates that the global parameter τ determines the extent to which we rely on the source estimate. In the context of standard horseshoe prior, Piironen and Vehtari (2017a,b) suggest to set $\tau = p_0/(p - p_0)\sigma$, where p_0 represents the prior guess for the number of non-zero variables in the coefficient. We take a similar approach to determine τ as stated in the below proposition with detailed justification in the supplement.

Proposition 1 (Determine τ through number of informative elements). *Define $\psi = \sum_{j=1}^p \kappa_j$, which essentially counts the number of informative elements in the p -dimensional source estimates. The expectation of ψ given τ is $\mathbb{E}(\psi \mid \tau) = p/(1 + \tau\sqrt{n_0})$. Given Equation*

(4) and our prior guess of ψ being $\hat{\psi}$, we can solve $\mathbb{E}(\psi \mid \tau) = \hat{\psi}$, leading to the solution $\tau_0 = (p - \hat{\psi})/(\sqrt{n_0}\hat{\psi})$.

Recall that κ_j is the element-wise shrinkage factor towards the source parameter. This makes ψ a natural indicator of how much information to leverage from the source. In this paper, we use $\hat{\psi} = p/2$, reflecting a prior belief that 50% of the elements in the final estimates borrow information from the source estimates.

Hyperpriors like the half-Cauchy distribution are commonly used for τ in standard horse-shoe models, but we do not recommend them in our framework. Such priors can cause τ to shrink excessively to zero in MCMC sampling, resulting in instability and overly narrow posterior credible intervals. This issue arises in our setting where the source estimates are close to the true values, requiring little adjustment to reach β^* . In contrast, this is less of a concern in standard continuous shrinkage priors with zero mean prior, as τ must remain large enough to ensure accurate posterior intervals for non-zero parameters.

3 Theory

In this section, we study the theoretical properties of TRADER. We demonstrate that by incorporating informative source information, TRADER achieves more accurate posterior concentration around the true coefficients than standard continuous shrinkage priors, effectively mitigating the undercoverage problem in standard continuous shrinkage prior. Moreover, when the sources are uninformative, TRADER is robust to prevent negative transfer and covers the standard continuous shrinkage priors as a special case.

Assumption 1. All the covariates are uniformly bounded. For simplicity, we assume that $\mathbf{x}_{ij} \in [-1, 1]$ where \mathbf{x}_{ij} denotes the element in the i -th row and the j -th column of $\mathbf{X}^{(0)}$. We also require that the dimension be high, so $p \gg n_0$.

Assumption 2. We assume that $s \log p \ll n_0$.

Assumption 3. There exists an integer \bar{p} such that $\bar{p} > s$, $\bar{p} \asymp s$, and a constant $\lambda_0 > 0$ satisfying $\lambda_{\min}(\mathbf{X}_\xi^{(0)\top} \mathbf{X}_\xi^{(0)}) \geq n_0 \lambda_0$ for all ξ with $|\xi| \leq \bar{p}$.

Assumption 1 imposes a minor condition on the covariates, while Assumptions 2-3 allow us to have identifiability of the model and develop statistical theory, see Song and Liang (2023). The first result below considers the single source setting, establishing conditions under which the source is helpful, and providing the posterior consistency of TRADER. For readability, in this section, we omit the superscript when referring to a single scaled source and denote the scaled source as $\tilde{\omega} = (\|\hat{\boldsymbol{\beta}}^{\text{val}}\| / \|\hat{\boldsymbol{\omega}}\|) \hat{\boldsymbol{\omega}}$.

Theorem 1 (Posterior contraction oracle inequality in single-source). Consider the linear regression model (1), where the design matrix $\mathbf{X}^{(0)}$ and the true $\boldsymbol{\beta}^*$ satisfy the Assumptions 1, 2 and 3. The prior for $\boldsymbol{\beta}$ and σ^2 is given by Equation (2) with fixed $\eta_1 = 1$. Next, let

$$\mathcal{A} := \left\{ r \geq 0 : r \leq C \min \left\{ \frac{1}{\sqrt{s}}, \sigma^* \left(\frac{\tilde{s}(r) \log p}{s^2 n_0} \right)^{1/4} \right\} \text{ and } \sum_{j: |\beta_j^* - \tilde{\omega}_j| \leq r} |\beta_j^* - \tilde{\omega}_j| \leq C \sqrt{\frac{\tilde{s}(r) \log p}{n_0}} \right\}$$

for a large enough constant $C > 0$ and where $\tilde{s}(r) = |\{j : |\beta_j^* - \tilde{\omega}_j| > r\}|$. Let $r_{\text{sup}} = \sup\{r : r \in \mathcal{A}\}$. Suppose that there exists $\gamma > 0$ such that $\|(\boldsymbol{\beta}^* - \tilde{\boldsymbol{\omega}})/\sigma^*\|_\infty \leq E := p^\gamma$ for some $\gamma > 0$. If τ satisfies $\tau \asymp p^{-u}$ for some appropriate $u > 0$, then for $\epsilon_n = M \sqrt{\tilde{s}(r_{\text{sup}}) \log p / n_0}$

for a large enough constant M , it holds that

$$\mathbb{P}^*(\pi(\|\widehat{\boldsymbol{\beta}} - \boldsymbol{\beta}^*\| \geq c_1 \sigma^* \epsilon_n | \mathcal{D}_0) \geq \exp(-c_2 n_0 \epsilon_n^2)) \leq \exp(-c_3 n_0 \epsilon_n^2),$$

for some positive constants c_1 , c_2 , and c_3 .

Remark 1. In Theorem 1, r_{sup} represents a threshold that provides relaxation to the usual notion of sparsity. The function $\tilde{s}(r)$ counts the number of coefficients $\tilde{\omega}_j$ whose deviation from β_j^* is greater than r , which measures how well $\tilde{\omega}$ approximates $\boldsymbol{\beta}^*$, with a larger r corresponding to fewer coefficients contributing to the sum. We choose r_{sup} to maximize r within \mathcal{A} because $\tilde{s}(r)$ decreases as r increases, meaning fewer coefficients violate the threshold as r grows. The constraint $r \in \mathcal{A}$ balances the approximation quality of $\tilde{\omega}$ to $\boldsymbol{\beta}$ with sparsity, based solely on differences $\tilde{\omega}_j - \beta_j$. The small r requirement arises from the proof, and $0 \in \mathcal{A}$ ensures $\tilde{s}(r_{\text{sup}}) \lesssim s + \text{sparsity of } \tilde{\omega}$. For settings where $\tilde{\omega}$ has $O(s)$ nonzero coefficients, we obtain $\tilde{s}(r) \lesssim s$. Thus, if $\tilde{\omega}$ reasonably estimates the sparsity of $\boldsymbol{\beta}^*$, the posterior contraction rate is no worse than when $\tilde{\omega} = 0$.

Corollary 1. Under the conditions of Theorem 1, if $\boldsymbol{\beta}^* - \tilde{\omega}$ is sparse in the sense that $s(\boldsymbol{\beta}^* - \tilde{\omega}) := |\{j : |\beta_j^* - \tilde{\omega}_j| \neq 0\}| \ll s$, then

$$\tilde{s}(r_{\text{sup}}) \leq s(\boldsymbol{\beta}^* - \tilde{\omega}) \ll s. \quad (5)$$

Hence, the posterior contraction rate is much faster than the original rate of target-only horseshoe (i.e., no source is used), thus

$$\sqrt{\frac{\tilde{s}(r_{\text{sup}}) \log p}{n_0}} \ll \sqrt{\frac{s \log p}{n_0}}.$$

If, in addition, many entries of $\boldsymbol{\beta}^* - \tilde{\omega}$ are small such that $\tilde{s}(r_{\text{sup}}) \ll s(\boldsymbol{\beta}^* - \tilde{\omega})$, then the

rate in Theorem 1 satisfies

$$\sqrt{\frac{\tilde{s}(r_{\text{sup}}) \log p}{n_0}} \ll \sqrt{\frac{s(\boldsymbol{\beta}^* - \tilde{\boldsymbol{\omega}}) \log p}{n_0}},$$

highlighting the usefulness of the oracle inequality established in Theorem 1.

Remark 2. Corollary 1 demonstrates the helpfulness of leveraging rescaled source estimate $\tilde{\boldsymbol{\omega}}$ in improving the posterior contraction rate, provided that $\tilde{\boldsymbol{\omega}}$ aligns well with the true parameter $\boldsymbol{\beta}^*$. It indicates that the closer $\tilde{\boldsymbol{\omega}}$ is to $\boldsymbol{\beta}^*$, both sparsely and in magnitude, the more significant the gains in posterior contraction rate, reinforcing the practical value of the oracle inequality in Theorem 1. Specifically, (1) If the differences between $\boldsymbol{\beta}^*$ and $\tilde{\boldsymbol{\omega}}$ are sparse, meaning that only a small number of entries in $\boldsymbol{\beta}^* - \tilde{\boldsymbol{\omega}}$ are non-zero, the effective sparsity parameter $\tilde{s}(r_{\text{sup}})$ is much smaller than s , leading to a faster posterior contraction rate; (2) When these differences are not only sparse but many are small in magnitude, the effective sparsity $\tilde{s}(r_{\text{sup}})$ becomes even smaller compared to $s(\boldsymbol{\beta}^* - \tilde{\boldsymbol{\omega}})$. This further enhances the posterior contraction rate, making it significantly faster than the rate when no source is used; and (3) These results highlight the utility of incorporating well-aligned source information. When $\tilde{\boldsymbol{\omega}}$ closely approximates $\boldsymbol{\beta}^*$, both in terms of sparsity and magnitude of differences, the model achieves much faster learning rates. This underscores the importance of selecting or constructing high-quality source information.

Our next result outlines conditions for ensuring posterior consistency in the presence of multiple sources, where the key condition (6) regulates the support magnitude when aggregating information across sources.

Theorem 2 (Posterior consistency with multiple sources that underestimate the support). Let $\tilde{\boldsymbol{\omega}}^{(1)}, \dots, \tilde{\boldsymbol{\omega}}^{(K)} \in \mathbb{R}^p$ be vectors learned from K source data, respectively,

independent of the target data. Suppose that

$$\max\{\|\mathbf{b}^*\|_\infty, K \max_{k=1,\dots,K} \|\tilde{\boldsymbol{\omega}}^{(k)}\|_\infty\} / \sigma^* \leq p^\gamma$$

for a positive constant γ . Consider the prior for $\boldsymbol{\beta}$ and σ_0^2 defined by Equation (2) with $\tau > 0$. Next, let $\tilde{\boldsymbol{\omega}} = \sum_{k=1}^K \eta_k^* \tilde{\boldsymbol{\omega}}^{(k)}$ for arbitrary $\eta_1^*, \dots, \eta_K^* \in [0, 1]$ such that $\sum_{k=1}^K \eta_k^* \leq 1$. Let $r \in \mathcal{A}$, where \mathcal{A} is as defined in Theorem 1, and suppose that for an appropriate constant $c > 0$,

$$|\{j \in \{1, \dots, p\} : \max_{k=1,\dots,K} |\tilde{\omega}_j^{(k)}| > 0\}| \leq c\tilde{s}(r). \quad (6)$$

If τ satisfies $\tau \asymp n_0^{-u}$ for some appropriate $u > 0$, then for $\epsilon_n = M\sqrt{\tilde{s}(r) \log p / n_0}$ for a large enough positive constant M , it holds that

$$\mathbb{P}^*(\pi(\|\hat{\boldsymbol{\beta}} - \boldsymbol{\beta}^*\| \geq c_1 \sigma^* \epsilon_n | \mathcal{D}_0) \geq \exp(-c_2 n_0 \epsilon_n^2)) \leq \exp(-c_3 n_0 \epsilon_n^2)$$

for some positive constants c_1 , c_2 , and c_3 .

Remark 3. Theorem 2 highlights the flexibility of combining multiple sources, even when each individually underestimates the support of $\boldsymbol{\beta}^*$. The weights $\eta_1^*, \dots, \eta_K^*$, determine how the rescaled sources $\tilde{\boldsymbol{\omega}}^{(1)}, \dots, \tilde{\boldsymbol{\omega}}^{(K)}$ are combined to approximate $\boldsymbol{\beta}^*$. While these weights are unknown, they can be arbitrary as long as the theorem's conditions are met, and an oracle with perfect knowledge of $\boldsymbol{\beta}^*$ could select the optimal weights to achieve the sharpest posterior contraction rate. Furthermore, Theorem 2 includes realistic scenarios where each source provides a partial view of the true support, capturing only a subset of the relevant nonzero coefficients in $\boldsymbol{\beta}^*$. By combining these sources with appropriately chosen weights, the model leverages their collective strength to better approximate $\boldsymbol{\beta}^*$, even when individual sources are noisy or incomplete. Moreover, the sparsity condition (6) ensures that the combined source information retains a sparse structure, enabling efficient and robust posterior contraction.

This makes the framework well-suited for high-dimensional settings, where reliable information is often spread across multiple sources. In the next result, we give more intuition about the actual upper bound.

Another interesting observation from Theorem 2 is that TRADER can account for the scenarios of partial information sharing discussed in Zhang et al. (2024), where sources underestimate the true support. Specifically, they assumed that $\tilde{\omega}_\xi^{(k)}$ closely resembles β_ξ only for some $\xi \in \{1, \dots, p\}$, while other covariates are uninformative. Under condition (6), this scenario is well-addressed by TRADER, as Theorem 2 demonstrates its ability to leverage source information even when individual $\tilde{\omega}^{(k)}$ underestimates the true parameter support.

Corollary 2. *Using the notation from Theorem 2, if we take $r = 0$, then $r \in \mathcal{A}$, and condition (6) becomes*

$$|\{j \in \{1, \dots, p\} : \min_{k=1, \dots, K} |\tilde{\omega}_j^{(k)}| > 0\}| \leq c |\{j : |\beta_j^* - \tilde{\omega}_j| > 0\}| := s(\eta^*), \quad (7)$$

since the weights $\eta_1^*, \dots, \eta_K^*$ determine $\tilde{\omega}$. Then the contraction rate can be expressed as

$$\sqrt{\frac{\log p}{n}} \cdot \inf_{\eta_1^*, \dots, \eta_K^* \in [0, 1], \sum_{k=1}^K \eta_k^* \leq 1, \eta^* \text{ satisfies (7)}} \sqrt{s(\eta^*)}.$$

If we take $\eta^* = 0$, then condition (7) becomes

$$|\{j \in \{1, \dots, p\} : \max_{k=1, \dots, K} |\tilde{\omega}_j^{(k)}| > 0\}| \leq cs, \quad (8)$$

and the corresponding contraction rate is $\sqrt{s \log p / n_0}$. Thus, under condition (8), the worst-case contraction error rate is the same as if no sources were used, i.e., target-only horseshoe.

Remark 4. *Corollary 2 highlights the role of weights $\eta_1^*, \dots, \eta_K^*$ in determining how the*

sources contribute to the contraction rate. When $r = 0$, the effective sparsity $s(\eta^*)$ reflects the overlap between the true support of $\boldsymbol{\beta}^*$ and the combined source information. A smaller $s(\eta^*)$ results in a faster contraction rate, showing the benefit of well-aligned sources. In the worst-case scenario where $\eta^* = 0$, i.e., no contribution from sources, the contraction rate reduces to the baseline $\sqrt{s \log p/n_0}$ (Song and Liang (2023)), equivalent to not using source information in the target-only estimate. This shows the robustness of TRADER by leveraging informative sources when available but not degrading when sources are unhelpful.

A notable observation from Theorems 1 and 2 is that TRADER can mitigate the undercoverage issue commonly observed in continuous shrinkage priors, provided at least one helpful source is available. To illustrate this, We first adopt a heuristic argument from Wu et al. (2023) to explain why standard continuous shrinkage priors often result in unsatisfactory coverage for signals with moderate signal strength, and then formally justify how TRADER addresses this limitation. Specifically, we express model (1) as

$$\mathbf{y}^{(0)} = \mathbf{x}_j^{(0)} \beta_j + \mathbf{X}_{-j}^{(0)} \boldsymbol{\beta}_{-j} + \boldsymbol{\epsilon}^{(0)},$$

where $\mathbf{X}_{-j}^{(0)}$ denotes $(\mathbf{x}_k^{(0)}, k \neq j)$ and $\boldsymbol{\beta}_{-j}$ represents $(\beta_1, \dots, \beta_{j-1}, \beta_{j+1}, \dots, \beta_p)^\top$. Based on Equation (3), the conditional distribution of $\boldsymbol{\beta}_{-j}$ given all other parameters is

$$\pi \left(\beta_j \mid \boldsymbol{\beta}_{-j}, \tau, \boldsymbol{\Lambda}, \mathbf{x}_j^{(0)}, \mathbf{X}_{-j}^{(0)}, \mathbf{y}^{(0)} \right) \propto \mathcal{N} \left(g_j \left(\widehat{\boldsymbol{\beta}}_{-j} \right), \sigma^2 \left(\mathbf{x}_j^{(0)\top} \mathbf{x}_j^{(0)} \right)^{-1} \right) \pi_{\beta_j}(\beta_j), \quad (9)$$

where $\pi_{\beta_j}(\beta_j)$ denotes a general continuous shrinkage prior on β_j . Because of the Bayesian estimation consistency, $\boldsymbol{\beta}_{-j}$ will convergence to $\boldsymbol{\beta}_{-j}^*$. The center of the marginal posterior of β_j 's will then approximately be $g_j(\widehat{\boldsymbol{\beta}}_{-j})$, where $\widehat{\boldsymbol{\beta}}_{-j}$ is the posterior of $\boldsymbol{\beta}_{-j}$ and $g_j(\widehat{\boldsymbol{\beta}}_{-j})$ is given by

$$g_j \left(\widehat{\boldsymbol{\beta}}_{-j} \right) = \underbrace{\beta_j^* + \left(\mathbf{x}_j^{(0)\top} \mathbf{x}_j^{(0)} \right)^{-1} \mathbf{x}_j^{(0)\top} \boldsymbol{\epsilon}^{(0)}}_{\text{MLE of } \beta_j} + \underbrace{\left(\mathbf{x}_j^{(0)\top} \mathbf{x}_j^{(0)} \right)^{-1} \mathbf{x}_j^{(0)\top} \mathbf{X}_{-j}^{(0)} \left(\boldsymbol{\beta}_{-j}^* - \widehat{\boldsymbol{\beta}}_{-j} \right)}_{\text{bias term}}. \quad (10)$$

When $\widehat{\boldsymbol{\beta}}_{-j} = \boldsymbol{\beta}_{-j}^*$, the first two terms of Equation (10) represent the maximum likelihood estimate (MLE) of $\boldsymbol{\beta}_j$ with the second term having order $O_p(\sqrt{1/n_0})$. For a standard continuous shrinkage prior, the issue of low coverage probability for moderate signals arises due to the last bias term, which is of order $O_p(\sqrt{(s \log(p-1))/n_0})$. This term dominates the remaining terms and cannot be captured by the $O_p(\sqrt{1/n_0})$ spread of the posterior.

We show in the following result that TRADER achieves reliable inference by balancing the contributions of source and target information, even in scenarios with large biases or misaligned sources. Moreover, it also provides theoretical justification for how TRADER addresses the undercoverage issue. For simplicity, we assume only one source is available.

Theorem 3 (Finite-sample marginal posterior behavior under single-source). *Suppose that $\sigma^{*2} = \sigma^2$ is known and consider the setting of Theorem 1 with no prior on σ^2 . Let $j \in \{1, \dots, p\}$ and $\sigma_j^2 = \sigma^2(\mathbf{x}_j^{(0)\top} \mathbf{x}_j^{(0)})^{-1}$. Assume that $\|\mathbf{x}_j^{(0)}\| \asymp \sqrt{n_0}$, and there exists $\bar{p} > \max\{\tilde{s}(r_{\text{sup}}), s\}$ and a constant $a_0 > 0$ such that*

$$\lambda_{\max} := \Lambda_{\max} \left(\frac{\mathbf{X}_{\xi}^{(0)\top} \mathbf{X}_{\xi}^{(0)}}{n_0} \right) < a_0$$

for all $\xi \subset \{1, \dots, p\}$ with $|\xi| < \bar{p}$. Let us also assume that $|\beta_j^* - \tilde{w}_j|^2 = o(\sigma p^2)$. Define

$$\mathcal{B} := \left\{ \boldsymbol{\beta}_{-j} : \left| \underbrace{\left(\mathbf{x}_j^{(0)\top} \mathbf{x}_j^{(0)} \right)^{-1} \mathbf{x}_j^{(0)\top} \mathbf{X}_{-j}^{(0)} (\boldsymbol{\beta}_{-j}^* - \boldsymbol{\beta}_{-j})}_{\text{bias term}} \right| \leq C_0 \sqrt{\frac{\tilde{s}(r_{\text{sup}}) \log p}{n}} \right\} \quad (11)$$

for some appropriate constant $C_0 > 0$. The following holds:

(i) Suppose $|\tilde{w}_j - \beta_j^*| > C\sigma\epsilon_n$ for some constant $C > 0$. Then, there exists a distribution F_j with support contained in \mathcal{B} such that the random variable β_j generated as

$$\begin{aligned} \beta_j | \boldsymbol{\beta}_{-j} &\sim \mathcal{N}(g_j(\boldsymbol{\beta}_{-j}), \sigma_j^2), \\ \boldsymbol{\beta}_{-j} &\sim F_j, \end{aligned} \quad (12)$$

has a marginal distribution f_j that satisfies

$$\|f_j - \pi(\beta_j | \mathcal{D}_0, \sigma^2)\|_{\text{TV}} = O\left(\frac{|\beta_j^* - \tilde{\omega}_j|^2}{\sigma p^2} + \exp(-c_2 n_0 \epsilon_n^2) + \frac{\sigma \epsilon_n}{|\beta_j^* - \tilde{\omega}_j|}\right) \quad (13)$$

with probability approaching one.

(ii) In contrast, if $|\tilde{\omega}_j - \beta_j^*| \leq C\sigma\epsilon_n$, then in the construction of $\beta_j | \boldsymbol{\beta}_{-j}$ in (12), we now have

$$p(\beta_j | \boldsymbol{\beta}_{-j}) \propto \mathcal{I}(\beta_j \in R(\boldsymbol{\beta}_{-j})) \mathcal{N}(\beta_j; g_j(\boldsymbol{\beta}_{-j}), \sigma_j^2) \cdot h(\beta_j),$$

where $\mathcal{I}(\beta_j \in R(\boldsymbol{\beta}_{-j}))$ is the indicator for the interval $R(\boldsymbol{\beta}_{-j}) = [g_j(\boldsymbol{\beta}_{-j}) - \tilde{C}\sigma\epsilon_n, g_j(\boldsymbol{\beta}_{-j}) + \tilde{C}\sigma\epsilon_n]$, with the constant $\tilde{C} > 0$ large enough such that $\tilde{\omega}_j \in R(\boldsymbol{\beta}_{-j})$. Moreover, the function h satisfies $\lim_{\beta_j \rightarrow \tilde{\omega}_j} h(\beta_j) = \infty$. Then, for the corresponding f_j , it holds that

$$\|f_j - \pi(\beta_j | \mathcal{D}_0, \sigma^2)\|_{\text{TV}} = o(1). \quad (14)$$

Remark 5. Theorem 3 describes the behavior of the posterior mean for each coefficient β_j under TRADER. When $|\tilde{\omega}_j - \beta_j^*| > C\sigma\epsilon_n$, we obtain a finite-sample result establishing that the marginal posterior for β_j can be approximated as $\mathcal{N}(\beta_j^*, \sigma_j^2) + \text{bias}$, where the bias term is guaranteed to satisfy $O(\sqrt{\tilde{s}(r_{\text{sup}}) \log p/n_0})$. Thus, if the sparsity level $s(r_{\text{sup}})$ is oracle-like, as stated in Theorem 1, TRADER's posterior centers around MLE with a diminishing bias that can be substantially smaller than $O(\sqrt{s \log p/n_0})$. This demonstrates TRADER's ability to leverage the overall informativeness of the source $\tilde{\boldsymbol{\omega}}$ to improve the estimation of β_j , even when $\tilde{\omega}_j$ deviates by at least $C\sigma\epsilon_n$, from the truth coefficient β_j^* .

In contrast, when $|\tilde{\omega}_j - \beta_j^*| < C\sigma\epsilon_n$, indicating that the source $\tilde{\boldsymbol{\omega}}$ is informative for the j -th coefficient, Theorem 3 indicates that the marginal posterior concentrates tightly around the true coefficient β_j^* , even if the bias remains at the order of $\sqrt{s \log p/n_0}$.

Remark 6. In TRADER, if at least one source estimate is informative, Theorems 1 and

2 establish conditions under which the fitting error of β_j converges faster than the usual $O(\sqrt{s \log p/n_0})$. Building on Theorem 3, TRADER achieves faster convergence through its adaptive guided structure, which prioritizes target-only information in the presence of large biases, i.e., $|\tilde{\omega}_j - \beta_j^*| \gg C\sigma\epsilon_n$, effectively mitigating the undercoverage issue in moderate signal strength scenarios. Thus, TRADER balances contributions from source and target information, ensuring robust coverage and reliable inference even in challenging cases of source misalignment or moderate signals.

4 Simulations

In this section, we conduct extensive simulation studies to evaluate the performance of TRADER. To ensure a comprehensive assessment, we stratify the results by signal and noise levels. We compare TRADER against the target-only model using the standard horseshoe prior, as well as TransGLM (Tian and Feng, 2023), a frequentist method that leverages multiple source datasets to construct confidence intervals for each coefficient under the assumption that individual-level data from all source datasets are available. Our objective is to assess whether TRADER can outperform the target-only model while achieving estimation accuracy comparable to frequentist transfer learning methods that rely on individual-level source data.

For each setting of K , we apply the standard horseshoe prior to the target data only as a baseline. The transfer learning methods differ in the data they can access. TransGLM uses the full individual-level data $\mathcal{D}^{(k)}$ from each source for model training. In contrast, since TRADER only requires pre-trained source models, we first apply the standard horseshoe

prior to all $\mathcal{D}^{(k)}$ to obtain the fitted model estimates, $\widehat{\omega}^{(k)}$. This summary data is then passed to TRADER for model training, mimicking the real-world situation where TRADER only needs source model estimates for implementation. TRADER is implemented using Stan (Stan Development Team, 2024). Additional simulation results are provided in the supplement. We repeat simulations in each setting 200 times unless otherwise specified.

We evaluate our model performance using six metrics, focusing on estimation accuracy and coverage of the true signal. For settings I and II, we use all six metrics, while for setting III, we use only the first three as β^* is not sparse: (1) Estimation mean squared error (MSE): defined as $\text{MSE} = (1/p) \sum_{j=1}^p (\widehat{\beta}_j^{\text{mean}} - \beta_j)^2$, where $\widehat{\beta}_j^{\text{mean}}$ is the posterior mean of β_j ; (2) Average width: the width of 95% credible/confidence interval averaged over all parameters; (3) Coverage: the proportion of the 95% credible/confidence interval that correctly captured the true value; (4) True Positive Rate (TPR): $\text{TP}/(\text{TP} + \text{FN})$, where True Positives (TP) are variables correctly selected as part of the true model, and False Negatives (FN) are variables that were incorrectly excluded despite being part of the true model; (5) True Negative Rate (TNR): $\text{TN}/(\text{TN} + \text{FP})$, where True Negatives (TN) are variables correctly excluded from the model, and False Positives (FP) are variables incorrectly included in the model; and (6) False Positive Rate (FPR): $\text{FP}/(\text{FP} + \text{FN})$, measuring the proportion of irrelevant variables incorrectly included in the model.

4.1 Setting I: All Sources Are Informative

In the first simulation setting, we assume that all sources are informative, meaning their coefficients are similar to those of the target dataset and provide valuable information for

improving uncertainty quantification in the target data. Specifically, the target dataset has a sample size of $n_0 = 120$ and a dimension of $p = 200$. The covariates for the target dataset $\mathbf{x}_i^{(0)}$ are simulated from a multivariate normal distribution $\mathcal{N}(\mathbf{0}_p, \mathbf{A})$, where $\mathbf{A} = [A_{jj'}]_{p \times p}$ and $A_{jj'} = 0.5^{|j-j'|}$, for all $i = 1, \dots, n_0$. The coefficients in the target dataset are set as $\boldsymbol{\beta} = (0.5 \times \mathbf{1}_s^\top, \mathbf{0}_{p-s}^\top)^\top$, where $\mathbf{1}_s$ has all s elements equal to 1 and $\mathbf{0}_{p-s}$ has all $(p-s)$ elements 0. We set $s = 20$ throughout our simulation.

The source datasets are set to have the same number of parameters as the target, with $K = 10$ sources. Each source dataset has a sample size of $n_k = 120$. We define $\mathcal{I}_p^{(k)}$ as p independent random variables, each taking a value of 1 or -1 with equal probability, for any source k . The random variable $\mathcal{I}_p^{(k)}$ is independent across sources. For source dataset k , we set $\omega_j^{(k)} = \beta_j + (h/p)\mathcal{I}_p^{(k)}$ with $h = 15$. The covariates for source k are generated from $\mathcal{N}(\mathbf{0}_p, \mathbf{A} + \boldsymbol{\epsilon}\boldsymbol{\epsilon}^\top)$ with $\boldsymbol{\epsilon} \sim \mathcal{N}(\mathbf{0}_p, 0.3^2\mathbf{I}_p)$ and are generated independently for each source.

Figure 2 shows that TRADER achieves significantly lower average estimation error for signal variables compared to the target-only horseshoe prior, as expected. This improvement arises because the TRADER prior incorporates information from source datasets, compensating for the limited sample size of the target dataset. Although TransGLM achieves an even lower estimation error due to access to individual-level data, Figure S1 shows that TRADER's estimation error for both signal and noise variables approaches that of TransGLM as K increases. A comparison between Figure 2 and S1 reveals that TRADER's advantage over the horseshoe prior primarily comes from enhanced estimation accuracy in signal variables.

As K increases, both TRADER's credible intervals and TransGLM's confidence intervals achieve the nominal 95% coverage for both signal and noise variables. Additionally, the

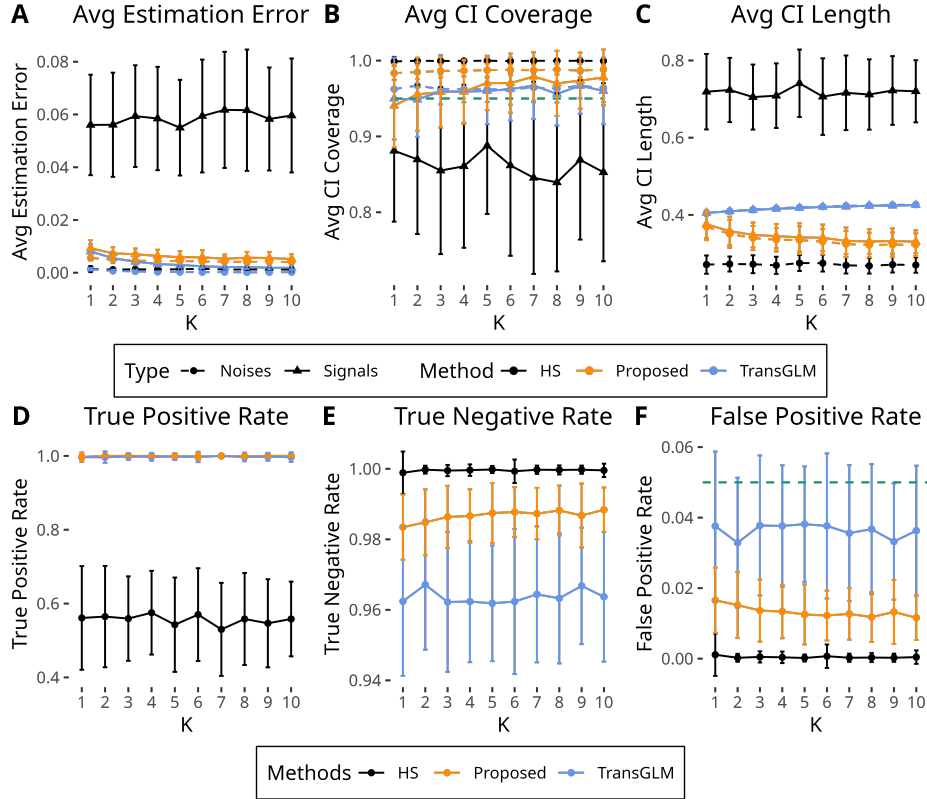


Figure 2: (Simulation Setting I) Comparison of TRADER, TransGLM, and standard horseshoe prior (HS) across different values of K , regarding (A) the average estimation error, (B) the average credible/confidence coverage, where the 95% level is denoted as the green dashed horizontal line, (C) the average credible/confidence interval length, (D) true positive rate, (E) true negative rate, and (F) false positive rate, where the green dashed line represents an FPR of 0.05. Parameters are set to $h = 15$, $n_0 = 120$ and $n_k = 120$ for all $K = 1, \dots, 10$, $p = 200$, $s = 20$. Error bars denote the standard deviations.

average length of TRADER’s credible intervals and TransGLM’s confidence intervals are significantly shorter than that of the horseshoe prior. Regarding TPR, TRADER performs comparably to TransGLM and significantly outperforms the target-only horseshoe prior. While all three methods exhibit similar TNR, TransGLM shows a higher FPR, close to 0.05, highlighting the benefits of transfer learning for more precise parameter estimates. Finally, TransGLM shows a slight increase in confidence interval length, attributed to TransGLM’s more accurate estimation of β^* .

While the coverage for noise variables is satisfactory across all three methods, the stan-

standard horseshoe prior yields narrow credible intervals for signal variables, resulting in poor coverage. TRADER does not exhibit this issue, supporting our argument in Section 3 that standard Bayesian shrinkage methods may fail to provide reliable uncertainty quantification with moderate signal strength, whereas TRADER remains effective. Furthermore, as shown in Figure ??, both TRADER and TransGLM perform well even when the signal strength is high enough for the horseshoe to reach nominal 95% coverage, highlighting the robustness of TRADER at different signal strengths.

We also evaluate TRADER’s performance under increasing heterogeneity between the source and target datasets. For $h = \{25, 35\}$, Figures S5 and S6 show that TRADER continues to outperform the target-only method and maintains comparable performance to TransGLM. This suggests that TRADER’s estimation remains robust even with substantial heterogeneity in the source datasets.

4.2 Setting II: Some but Unknown Sources Are Informative

In setting II, we assume that only a subset of the $K = 10$ sources are informative, but it is unknown which ones are informative. Since TRADER is designed to automatically downweight source estimates that are uninformative for the target dataset, we are particularly interested in evaluating its ability to safeguard against uninformative sources while successfully extracting information from informative sources.

We use the same data generation mechanism as setting I to generate the target dataset, except that the covariates $\mathbf{x}_i^{(0)} \sim \mathcal{N}(\mathbf{0}_p, \mathbf{B})$, where \mathbf{B} is a $p \times p$ matrix with entries $B_{jj'} = 0.9^{|j-j'|}$. For the source datasets, the covariates $\mathbf{x}_i^{(k)} \stackrel{\text{iid}}{\sim} \text{student} - t_4$ for $k = 1, \dots, K$. In the

case of the k -th informative source dataset, we set $\omega_j^{(k)} = \beta_j + (h/p)\mathcal{I}_p^{(k)}$ for $k = 1, \dots, K_a$.

For the remaining $K - K_a$ uninformative sources, we randomly select a subset $\mathcal{S}^{(k)}$ of size s from the range $\{2s + 1, \dots, p\}$. Then, the j -th component of $\omega^{(k)}$ is assigned as follows:

$$\omega_j^{(k)} = \begin{cases} 0.5 + 2h\mathcal{I}_j^{(k)}/p, & j \in \{s + 1, \dots, 2s\} \cup \mathcal{S}^{(k)}, \\ 2h\mathcal{I}_j^{(k)}/p, & \text{otherwise.} \end{cases}$$

In other words, for indices $j \in \{s + 1, \dots, 2s\}$ and those randomly chosen from the set $\{2s + 1, \dots, p\}$, we add 0.5 to the corresponding $\omega_j^{(k)}$. Lastly, for each source dataset, we include an intercept term of 0.5 in the response variable. The data generation process for each source dataset is independent of the others. We assume that K_a sources are informative, while the remaining sources are not. Neither TransGLM nor TRADER are aware of the informativeness of the source dataset in advance.

Figures 3 and S2 in the supplement show that, even with uninformative sources, TRADER performs similarly to TransGLM and outperforms the horseshoe prior. This is expected, as TRADER effectively extracts information from the sources. Its performance is comparable to TransGLM, indicating that TRADER's prior design recovers informative sources. As K_a increases, TRADER's estimation error and average credible interval length decrease. Both TransGLM and TRADER improve estimation by leveraging information from the sources. Overall, these results suggest that TRADER downweights uninformative sources and performs similarly to TransGLM.

As sensitivity analyses, we vary the signal strength of β and heterogeneity h of source datasets in additional simulations in the supplement. Figure S4 indicates that both TransGLM and TRADER achieve lower average estimation errors under different signal strengths. Additionally, Figures S7 and S8 show that TRADER is robust even when the differences

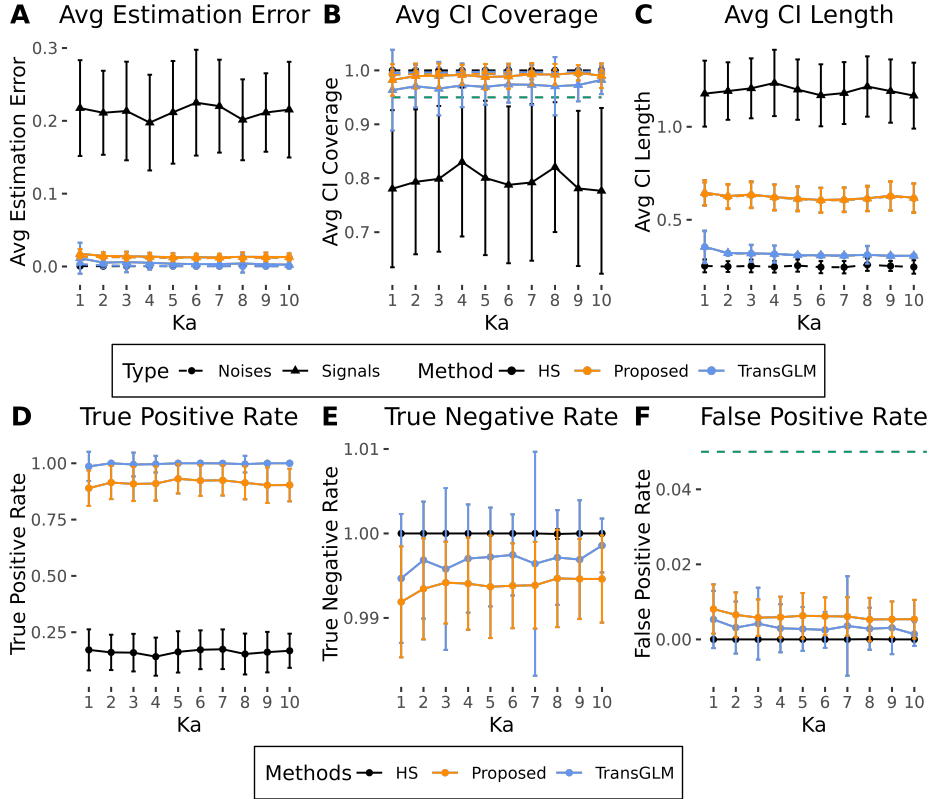


Figure 3: (Simulation setting II) Comparison of TRADER, TransGLM, and standard horseshoe prior (HS) regarding (A) the average estimation error, (B) the average credible/confidence coverage, where the 95% level is denoted as the green dashed horizontal line, (C) the average credible/confidence interval length, (D) true positive rate, (E) true negative rate, and (F) false positive rate, where the green dashed line represents an FPR of 0.05, with increasing K_a when $K = 10$. $h = 15$, $n_0 = 120$ and $n_k = 120$ for all $k = 1, \dots, 10$, $p = 200$, $s = 20$. Error bars denote the standard deviations.

between sources and the target are relatively large, and no prior knowledge on the informativeness of the sources is available.

4.3 Setting III: Source with Different Correlations and Scales

In setting III, we evaluate TRADER’s inference performance when incorporating sources with different scales relative to the target parameter, by varying the correlations and scales between the target and source estimates. We consider (1) source estimates with different scales from the target but fixed correlations, and (2) source estimates with moderate or

weak correlations with the target, while keeping the scale fixed. Notably, simulations I and II represent special cases of this setting, where the scales of $\boldsymbol{\beta}$ and $\boldsymbol{\omega}^{(k)}$ are similar, with correlations close to one for informative sources and zero for uninformative sources.

For $j \in \{1, \dots, p\}$, we generate

$$\left(\beta_j, \omega_j^{(1)}, \omega_j^{(2)}, \dots, \omega_j^{(K)} \right)^\top \stackrel{\text{iid}}{\sim} \mathcal{N} \left(\mathbf{0}_{K+1}, \frac{1}{p} \begin{pmatrix} \alpha_t^2 & \rho_1 \alpha_t \alpha_{s1} & \rho_2 \alpha_t \alpha_{s2} & \cdots & \rho_K \alpha_t \alpha_{sK} \\ \rho_1 \alpha_t \alpha_{s1} & \alpha_{s1}^2 & 0 & \cdots & 0 \\ \rho_2 \alpha_t \alpha_{s2} & 0 & \alpha_{s2}^2 & \cdots & 0 \\ \vdots & \vdots & \vdots & \ddots & \vdots \\ \rho_K \alpha_t \alpha_{sK} & 0 & 0 & \cdots & \alpha_{sK}^2 \end{pmatrix} \right),$$

where $\alpha_t = \mathbb{E} \|\boldsymbol{\beta}\|^2$ and $\alpha_{sk} = \mathbb{E} \|\boldsymbol{\omega}^{(k)}\|^2$ for $k = 1, \dots, K$, ρ_k is the correlation between $\boldsymbol{\beta}$ and $\boldsymbol{\omega}^{(k)}$. The covariates and responses of source and target datasets are generated in the same way as setting I. We vary the scale ratios as α_t/α_{sk} and correlations ρ_k . Specifically, setting (i) corresponds to scenario (1), where $\alpha_t/\alpha_{sk} = (1, 1.11, 1.22, 1.33, 1.44, 1.56, 1.66, 1.78, 1.89, 2)$, and settings (ii) and (iii) correspond to scenario (2), where (ii) considers $\alpha_t/\alpha_{sk} = 1$, $\rho_k = 0.7 \times \mathbf{1}_K$, and (iii) assumes $\alpha_t/\alpha_{sk} = 1$, $\rho_k = 0.2 \times \mathbf{1}_K$.

According to Figure 4(i), TRADER's average estimation error decreases progressively as the number of source K grows, and is consistently lower than applying standard horse-shoe prior to target data only. This suggests that TRADER effectively leverages additional sources to improve estimation accuracy, even when these sources have a different scale than the target. In contrast, although TransGLM's average estimation error also decreases with increasing K , its performance is inferior to that of TRADER, indicating that TransGLM is more sensitive to scale discrepancies between source and target estimates.

In Figures 4(ii) and (iii), we fix the scale ratios at one to evaluate TRADER's ability to

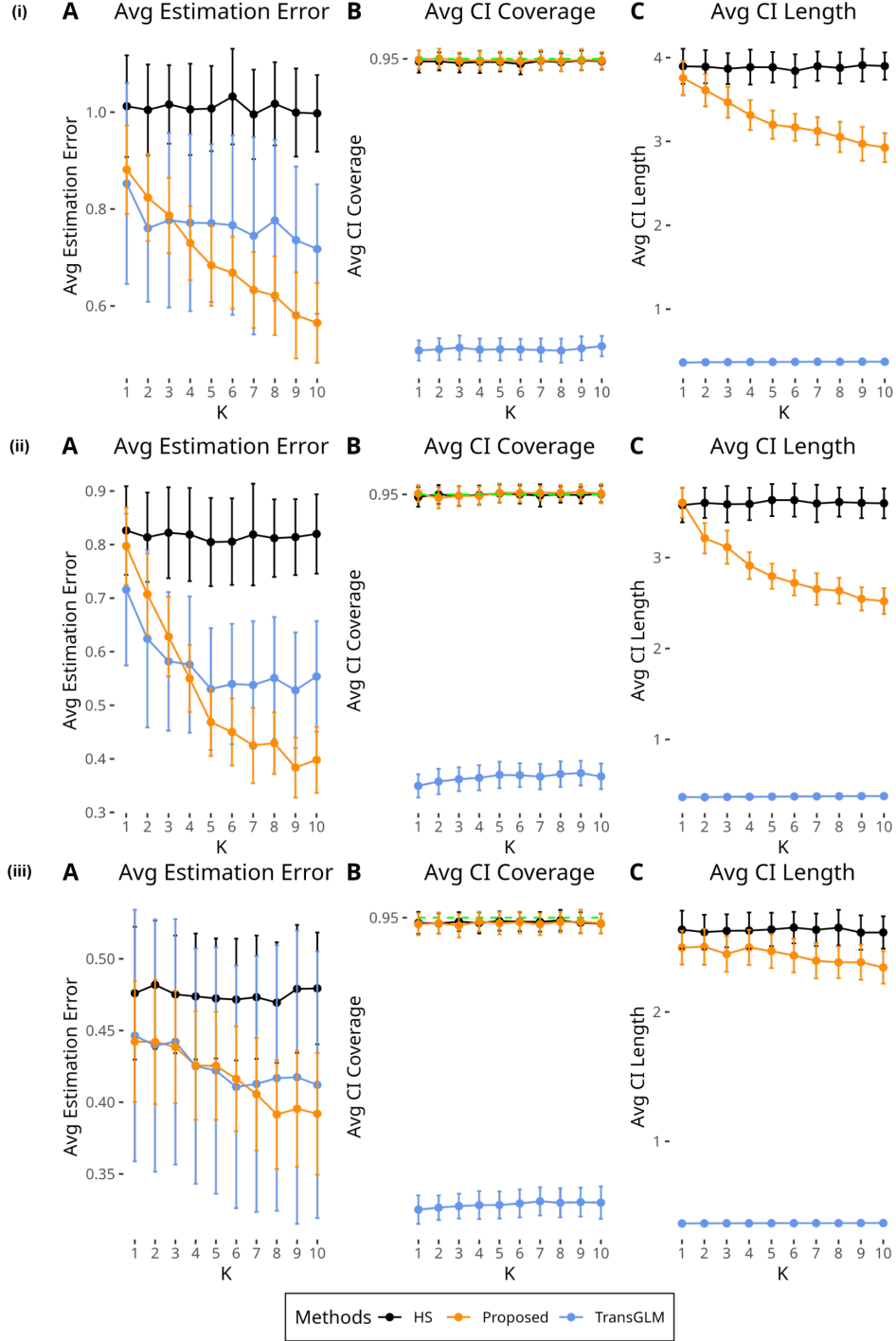


Figure 4: (Simulation setting III) Comparison of TRADER, TransGLM, and the target-only estimates via standard horseshoe prior (HS) regarding (A) the average estimation error, (B) the average credible/confidence coverage (the 95% level is denoted as the green dashed horizontal line), and (C) the average credible/confidence interval length. In each panel, for $k = 1, \dots, K$, (i) $\alpha_t/\alpha_{sk} = (1, 1.11, 1.22, 1.33, 1.44, 1.56, 1.66, 1.78, 1.89, 2)$, $\rho_k = 0.7 \times \mathbf{1}_K$, (ii) $\alpha_t/\alpha_{sk} = 1$, $\rho_k = 0.7 \times \mathbf{1}_K$, and (iii) $\alpha_t/\alpha_{sk} = 1$, $\rho_k = 0.2 \times \mathbf{1}_K$. Error bars denote the standard deviations.

utilize sources with varying correlations to the target. Figure 4(ii) indicates that TRADER’s average estimation error consistently decreases with more sources, while TransGLM initially reduces error but then sees a slight increase as K grows. Additionally, TransGLM’s confidence interval coverage drops significantly below the nominal 95% level. Figure 4(iii) demonstrates that even with small ρ_k ’s, TRADER still achieves marginal improvements in estimation error and credible interval length compared to the target-only horseshoe. In other words, TRADER can safeguard against negative transfer, preventing performance worse than using target data only. In contrast, while TransGLM shows a similar estimation error, its performance is less stable, and its average coverage probability decreases significantly compared to others.

In summary, the simulation shows TRADER effectively extracts useful information from source datasets with different scales or correlations compared to the target estimate, whereas TransGLM’s estimation performance is negatively impacted in such scenarios.

5 Real-Data Application

We apply TRADER to evaluate the relationship between HbA1C levels and long-term use of insulin among Hispanic individuals with diabetes. It is well-known that insulin usage reduces glucose levels, and this has been thoroughly studied and implemented in clinics for diverse racial and ethnic groups (Ford et al., 2019). We use the publicly available Medical Information Mart for Intensive Care (MIMIC-III) dataset (Johnson et al., 2016), treating HbA1C as the outcome of interest and insulin usage status as the covariate of interest. The data process details are in the Supplement. After quality control filtering, the final dataset

consists of two major ethnic groups: Caucasian ($n = 2,894$) and Hispanic ($n = 189$), with $p = 121$ covariates (see demographics in Table S1 in the supplement).

We follow the data extraction pipeline described by [Anand et al. \(2018\)](#). We included patients diagnosed with diabetes based on International Classification of Diseases (ICD) codes (250.0–259.0, diabetes). The HbA1C levels are extracted using LOINC code “4548-4”, excluding those missing HbA1C values. Demographic covariates, including patient gender, alcohol consumption, insurance type, marital status, ICU admission type, and ICU admission location, are extracted and included as covariates. Other patient diagnoses are filtered by excluding covariates that (i) have over 0.98 correlation with the insulin usage status, (ii) missing or unknown race information, and (iii) have no variation, i.e., all zeros.

As shown in Table 1, when looking at specific population groups, we find a significant association in Caucasians ($\beta_{\text{insulin}} = -1.091$, 95% confidence interval $[-1.349, -0.132]$). However, when we only consider the Hispanic population, the OLS estimation did not show any significant association ($\beta_{\text{insulin}} = -1.801$, 95% confidence interval $[-3.664, 0.063]$). This disparity, potentially resulting from unequal sample sizes across populations, motivates us to investigate whether integrating data from other populations could enhance estimates for Hispanics. Then, we apply TRADER to the Hispanic population by leveraging OLS estimates from African American and Caucasian populations as two independent source estimates. The results of TRADER indicate a strong association for Hispanics ($\beta_{\text{insulin}} = -1.064$, 95% credible interval $[-1.276, -0.843]$) and are consistent with the OLS estimate derived solely from the Hispanic population and provide a more precise measure of uncertainty for the current estimate. The results indicate that TRADER can effectively identify true biological associations, which is particularly beneficial in improving the estimation of risk factors in

underrepresented populations where biomedical data is often limited.

	Estimate (95% CI)	Significance
Caucasian-only (Source-only)	-1.091(-1.349, -0.132)	Yes
Hispanic-only (Target-only)	-1.801(-3.664, 0.063)	No
TRADER	-1.064(-1.276, -0.843)	Yes

Table 1: Effect size estimate and significance of insulin consumption in patients with diabetes over different models.

6 Discussion

In this paper, we introduce TRADER, a Bayesian transfer learning method via the guided horseshoe prior. This work offers new insights into the Bayesian transfer learning framework, particularly in leveraging source information to address the challenges posed by multiple, individual-level data-restricted, and unequally scaled source studies. It also addresses the gap in improving high-dimensional inference in a target population. Simulation studies reveal that existing transfer learning methods often fail when source and target datasets differ in scale or correlation structure. In contrast, TRADER overcomes these limitations by providing valid credible intervals for coefficient estimates, ensuring robust quantification of estimation uncertainty regardless of the signal strength. Additionally, we demonstrate its applicability and effectiveness in a real-data application to improve the estimation of blood glucose-related outcomes.

While TRADER enhances estimation in most cases, its performance relies on the informativeness of the source estimates. If the source data significantly differs from the target

or if the source estimates are biased—such as those obtained using frequentist methods like LASSO or elastic net—the benefits of transfer learning may diminish. To address this, if possible, such as in collaborative settings with source studies, we recommend recalculating source model parameters using debiased methods or proper Bayesian approaches to reduce bias. In this study, we use the standard horseshoe prior to obtain the source estimates. Other alternatives, such as debiased LASSO ([Zhang and Zhang, 2014](#)), can also be explored.

Although this study focuses on linear regression, the framework of TRADER is highly adaptable and can be extended to generalized linear models, allowing for broader application in real-world settings. Moreover, TRADER can be easily extended to provide prediction uncertainty, tailored to the specific study goals. Furthermore, the use of source-guided continuous shrinkage prior introduced in TRADER can be integrated into other Bayesian continuous priors ([Bhattacharya et al., 2015](#); [Bhadra et al., 2017](#); [Ročková, 2018](#); [Bai and Ghosh, 2019](#); [Zhang et al., 2022](#); [Li et al., 2024](#)), offering a flexible tool for diverse inference and prediction tasks.

Future work could focus on extending TRADER to non-linear models, such as kernel regression, to capture more complex associations between covariates and outcomes, or applying it to time-to-event outcomes in survival analysis. Another potential direction is adapting TRADER to handle heterogeneous covariates between source and target datasets, which is particularly relevant in multi-center studies where different hospitals may collect varying sets of patient information.

References

- Abba, M. A., Williams, J. P., and Reich, B. J. (2024). A Bayesian shrinkage estimator for transfer learning. *arXiv preprint arXiv:2403.17321*.
- Al-Stouhi, S. and Reddy, C. K. (2016). Transfer learning for class imbalance problems with inadequate data. *Knowledge and Information Systems*, 48:201–228.
- Anand, R. S., Stey, P., Jain, S., Biron, D. R., Bhatt, H., Monteiro, K., Feller, E., Ranney, M. L., Sarkar, I. N., and Chen, E. S. (2018). Predicting mortality in diabetic ICU patients using machine learning and severity indices. *American Medical Informatics Association Summits on Translational Science Proceedings*, 2018:310.
- Bai, R. and Ghosh, M. (2019). Large-scale multiple hypothesis testing with the normal-beta prime prior. *Statistics*, 53(6):1210–1233.
- Bastani, H. (2021). Predicting with proxies: Transfer learning in high dimension. *Management Science*, 67(5):2964–2984.
- Bhadra, A., Datta, J., Polson, N. G., and Willard, B. (2017). The Horseshoe+ Estimator of Ultra-Sparse Signals. *Bayesian Analysis*, 12(4):1105 – 1131.
- Bhadra, A., Datta, J., Polson, N. G., and Willard, B. (2019). Lasso Meets Horseshoe: A Survey. *Statistical Science*, 34(3):405 – 427.
- Bhattacharya, A., Pati, D., Pillai, N. S., and Dunson, D. B. (2015). Dirichlet–laplace priors for optimal shrinkage. *Journal of the American Statistical Association*, 110(512):1479–1490.

- Cai, T., Li, M., and Liu, M. (2024). Semi-supervised triply robust inductive transfer learning. *Journal of the American Statistical Association*, (just-accepted):1–22.
- Cai, T., Liu, M., and Xia, Y. (2022). Individual data protected integrative regression analysis of high-dimensional heterogeneous data. *Journal of the American Statistical Association*, 117(540):2105–2119.
- Carvalho, C. M., Polson, N. G., and Scott, J. G. (2009). Handling sparsity via the horseshoe. In *Artificial Intelligence and Statistics*, pages 73–80. PMLR.
- Carvalho, C. M., Polson, N. G., and Scott, J. G. (2010). The horseshoe estimator for sparse signals. *Biometrika*, 97(2):465–480.
- Chatterjee, N., Chen, Y.-H., Maas, P., and Carroll, R. J. (2016). Constrained maximum likelihood estimation for model calibration using summary-level information from external big data sources. *Journal of the American Statistical Association*, 111(513):107–117.
- Chen, E., Chen, X., Jing, W., and Zhang, Y. (2024). Distributed tensor principal component analysis. *arXiv preprint arXiv:2405.11681*.
- Cheng, W., Taylor, J. M., Gu, T., Tomlins, S. A., and Mukherjee, B. (2019). Informing a risk prediction model for binary outcomes with external coefficient information. *Journal of the Royal Statistical Society Series C: Applied Statistics*, 68(1):121–139.
- Duan, R., Boland, M. R., Moore, J. H., and Chen, Y. (2018). Odal: A one-shot distributed algorithm to perform logistic regressions on electronic health records data from multiple clinical sites. In *BIOCOMPUTING 2019: Proceedings of the Pacific Symposium*, pages 30–41. World Scientific.

- Duan, R., Luo, C., Schuemie, M. J., Tong, J., Liang, C. J., Chang, H. H., Boland, M. R., Bian, J., Xu, H., Holmes, J. H., et al. (2020). Learning from local to global: An efficient distributed algorithm for modeling time-to-event data. *Journal of the American Medical Informatics Association*, 27(7):1028–1036.
- Duan, R., Ning, Y., and Chen, Y. (2022). Heterogeneity-aware and communication-efficient distributed statistical inference. *Biometrika*, 109(1):67–83.
- Ford, C. N., Leet, R. W., Kipling, L., Rhee, M. K., Jackson, S. L., Wilson, P. W., Phillips, L. S., and Staimez, L. R. (2019). Racial differences in performance of HbA1c for the classification of diabetes and prediabetes among US adults of non-Hispanic black and white race. *Diabetic Medicine*, 36(10):1234–1242.
- Gao, B. and Zhou, X. (2024). MESuSiE enables scalable and powerful multi-ancestry fine-mapping of causal variants in genome-wide association studies. *Nature Genetics*, 56(1):170–179.
- Gu, T., Han, Y., and Duan, R. (2022a). Robust angle-based transfer learning in high dimensions. *arXiv preprint arXiv:2210.12759*.
- Gu, T., Han, Y., and Duan, R. (2022b). A transfer learning approach based on random forest with application to breast cancer prediction in underrepresented populations. In *PACIFIC SYMPOSIUM ON BIOCOMPUTING 2023: Kohala Coast, Hawaii, USA, 3–7 January 2023*, pages 186–197. World Scientific.
- Gu, T., Lee, P. H., and Duan, R. (2023a). COMMUTE: communication-efficient transfer learning for multi-site risk prediction. *Journal of Biomedical Informatics*, 137:104243.

- Gu, T., Li, S., and Duan, R. (2024). On the equivalence of transfer learning methods. *arXiv preprint*.
- Gu, T., Taylor, J. M., Cheng, W., and Mukherjee, B. (2019). Synthetic data method to incorporate external information into a current study. *Canadian Journal of Statistics*, 47(4):580–603.
- Gu, T., Taylor, J. M., and Mukherjee, B. (2023b). A meta-inference framework to integrate multiple external models into a current study. *Biostatistics*, 24(2):406–424.
- Gu, T., Taylor, J. M. G., and Mukherjee, B. (2023c). A synthetic data integration framework to leverage external summary-level information from heterogeneous populations. *Biometrics*, 79(4):3831–3845.
- Han, P. and Lawless, J. F. (2019). Empirical likelihood estimation using auxiliary summary information with different covariate distributions. *Statistica Sinica*, 29(3):1321–1342.
- Han, P., Taylor, J. M., and Mukherjee, B. (2023). Integrating information from existing risk prediction models with no model details. *Canadian Journal of Statistics*, 51(2):355–374.
- Hector, E. C. and Martin, R. (2024). Turning the information-sharing dial: efficient inference from different data sources. *Electronic Journal of Statistics*, 18(2):2974–3020.
- Hickey, J., Williams, J. P., and Hector, E. C. (2024). Transfer Learning with Uncertainty Quantification: Random Effect Calibration of Source to Target (RECaST). *Journal of Machine Learning Research*, 25(338):1–40.

- Ishwaran, H. and Rao, J. S. (2005). Spike and slab variable selection: Frequentist and Bayesian strategies. *The Annals of Statistics*, 33(2):730 – 773.
- Javanmard, A. and Montanari, A. (2014). Confidence intervals and hypothesis testing for high-dimensional regression. *Journal of Machine Learning Research*, 15(1):2869–2909.
- Jin, H. and Yin, G. (2021). Unit information prior for adaptive information borrowing from multiple historical datasets. *Statistics in Medicine*, 40(25):5657–5672.
- Johnson, A. E., Pollard, T. J., Shen, L., Lehman, L.-w. H., Feng, M., Ghassemi, M., Moody, B., Szolovits, P., Anthony Celi, L., and Mark, R. G. (2016). MIMIC-III, a freely accessible critical care database. *Scientific Data*, 3(1):1–9.
- Li, K.-C. (1989). Honest confidence regions for nonparametric regression. *The Annals of Statistics*, 17(3):1001–1008.
- Li, S., Cai, T., and Duan, R. (2023a). Targeting underrepresented populations in precision medicine: A federated transfer learning approach. *The Annals of Applied Statistics*, 17(4):2970–2992.
- Li, S., Cai, T. T., and Li, H. (2022). Transfer learning for high-dimensional linear regression: Prediction, estimation and minimax optimality. *Journal of the Royal Statistical Society Series B: Statistical Methodology*, 84(1):149–173.
- Li, S., Zhang, L., Cai, T. T., and Li, H. (2023b). Estimation and inference for high-dimensional generalized linear models with knowledge transfer. *Journal of the American Statistical Association*, pages 1–12.

- Li, X., Sham, P. C., and Zhang, Y. D. (2024). A Bayesian fine-mapping model using a continuous global-local shrinkage prior with applications in prostate cancer analysis. *The American Journal of Human Genetics*, 111(2):213–226.
- Lu, Y., Gu, T., and Duan, R. (2024). Enhancing genetic risk prediction through federated semi-supervised transfer learning with inaccurate electronic health record data. *Statistics in Biosciences*, pages 1–22.
- Miglioretti, D. L. (2003). Latent transition regression for mixed outcomes. *Biometrics*, 59(3):710–720.
- Need, A. C. and Goldstein, D. B. (2009). Next generation disparities in human genomics: concerns and remedies. *Trends in Genetics*, 25(11):489–494.
- Piironen, J. and Vehtari, A. (2017a). On the hyperprior choice for the global shrinkage parameter in the horseshoe prior. *Artificial Intelligence and Statistics*, pages 905–913.
- Piironen, J. and Vehtari, A. (2017b). Sparsity information and regularization in the horseshoe and other shrinkage priors. *Electronic Journal of Statistics*, 11(2):5018 – 5051.
- Polson, N. G. and Scott, J. G. (2011). Shrink Globally, Act Locally: Sparse Bayesian Regularization and Prediction. In *Bayesian Statistics 9*. Oxford University Press.
- Ročková, V. (2018). Bayesian estimation of sparse signals with a continuous spike-and-slab prior. *The Annals of Statistics*, 46(1):401 – 437.
- Schaid, D. J., Chen, W., and Larson, N. B. (2018). From genome-wide associations to

- candidate causal variants by statistical fine-mapping. *Nature Reviews Genetics*, 19(8):491–504.
- Song, Q. and Liang, F. (2023). Nearly optimal Bayesian shrinkage for high-dimensional regression. *Science China Mathematics*, 66(2):409–442.
- Stan Development Team (2024). Stan modeling language users guide and reference manual, version 2.35.
- Suder, P. M., Xu, J., and Dunson, D. B. (2023). Bayesian transfer learning. *arXiv preprint arXiv:2312.13484*.
- Taylor, J. M., Choi, K., and Han, P. (2023). Data integration: exploiting ratios of parameter estimates from a reduced external model. *Biometrika*, 110(1):119–134.
- Tian, Y. and Feng, Y. (2023). Transfer learning under high-dimensional generalized linear models. *Journal of the American Statistical Association*, 118(544):2684–2697.
- van de Geer, S., Bühlmann, P., Ritov, Y., and Dezeure, R. (2014). On asymptotically optimal confidence regions and tests for high-dimensional models. *The Annals of Statistics*, 42(3):1166 – 1202.
- van der Pas, S., Szabó, B., and van der Vaart, A. (2017). Uncertainty Quantification for the Horseshoe (with Discussion). *Bayesian Analysis*, 12(4):1221 – 1274.
- Wu, T., N. Narisetty, N., and Yang, Y. (2023). Statistical inference via conditional Bayesian posteriors in high-dimensional linear regression. *Electronic Journal of Statistics*, 17(1):769–797.

- Zhai, Y. and Han, P. (2022). Data integration with oracle use of external information from heterogeneous populations. *Journal of Computational and Graphical Statistics*, 31(4):1001–1012.
- Zhang, C.-H. and Zhang, S. S. (2014). Confidence intervals for low dimensional parameters in high dimensional linear models. *Journal of the Royal Statistical Society Series B: Statistical Methodology*, 76(1):217–242.
- Zhang, H. and Yin, G. (2023). Unit information prior for incorporating real-world evidence into randomized controlled trials. *Statistical Methods in Medical Research*, 32(2):229–241.
- Zhang, R., Zhang, Y., Qu, A., Zhu, Z., and Shen, J. (2024). CONCERT: Covariate-elaborated robust local information transfer with conditional spike-and-slab prior. *arXiv preprint arXiv:2404.03764*.
- Zhang, Y. D., Naughton, B. P., Bondell, H. D., and Reich, B. J. (2022). Bayesian regression using a prior on the model fit: The R2-D2 shrinkage prior. *Journal of the American Statistical Association*, 117(538):862–874.